CHEMISTRY OF MATERIALS

ARTICLE

pubs.acs.org/cm

Surface-Grafted Rodlike Polymers: Adaptive Self-Assembled Monolayers and Rapid Photo-Patterning of Surfaces

Mingu Han, M. Shahinur Rahman, Jae-Suk Lee, Dongyoon Khim, Dong-Yu Kim, and Ji-Woong Park*

School of Materials Science and Engineering, Gwangju Institute of Science and Technology, 261 Cheomdan-gwagiro, Buk-Gu, Gwangju 500-712, Korea

Supporting Information

ABSTRACT: We present a new concept of functionalizing solid surfaces using polymeric self-assembled monolayers (PSAM) that are obtained by grafting onto solid surfaces an asymmetric block copolymer composed of a long rodlike block and a short surface-reactive block. Poly(n-hexylisocyanate)-*b*-poly[3-(trimethoxysilyl) propyl methacrylate] (PHIC-*b*-PTMSM) is synthesized via a living anionic polymerization and an atom transfer radical polymerization. The new rod−coil block copolymer forms a polymeric self-assembled monolayer (PSAM) through covalent bonding of the sticky PTMSM block and planar adsorption of PHIC rodlike chains onto the substrate surface. The uniform PSAM with a thickness identical to the diameter of the rodlike chain is produced by the immersion coating method in a range of immersion solution concentrations and coating times. The PSAMs present unique properties thanks to the freedom of rotation of the end-grafted rodlike chains. The PSAMs exhibit nematic liquid crystalline ordering when the monolayer is fluidized by solvent vapor. A mixed SAM with a nanodot pattern is obtained by introducing a second coating agent of octadecyltrimethoxysilanes (ODTMS) onto the PSAM-coated substrate. The PSAM is micropatternable using photochemical cleavage of the anchoring blocks by brief exposure to UV. Use of the PSAMs as an additional dielectric layer in P3HT-based field effect transistors (FETs) is also demonstrated.

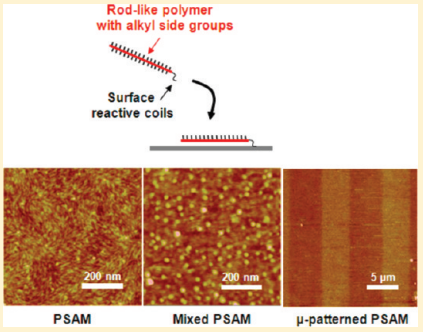

KEYWORDS: self-assembled monolayer (SAM), rod−coil diblock copolymer, mixed SAM, micropatterning, field effect transistors (FETs)

INTRODUCTION

Self-assembled monolayers (SAMs) are thin condensed layers formed by amphiphilic organic molecules adsorbed directly onto solid surfaces, and they provide an effective means for tailoring the properties and functions of solid surfaces.[1−3] SAM-forming organic molecules contain functional groups that are reactive or have a high affinity for the substrate surface onto which the SAM is prepared. The SAM molecules isolate the substrate surface from the air or fluid medium, and the surface properties of the SAMs are determined by the chemical nature of the moieties exposed to the air or fluid medium.[4−6]

SAMs can be prepared from small molecule or polymeric amphiphiles. Polymeric self-assembled monolayers (PSAM) offer a wide range of surface properties that cannot be obtained from small molecule SAMs.[7−10] Homo- or copolymerization of monomers or combinations of monomers permits tuning of the amphiphiles' chemical structure and the nature of surface attachment.[11−14] Ultrathin PSAMs may be prepared that display a variety of polymer physical properties: rigid or flexible conformations; crystalline, liquid-crystalline, rubbery, or amorphous phases; copolymer architectures; and phase separation behavior.[15−20] In particular, PSAMs exhibit stimuli-responsive properties if the polymer conformations and organizing structures are responsive to external stimuli such as temperature change,[21−23] solvent type,[24−27] and pH change.[28,29]

A polymer chain can be grafted to the surface in various ways; it can be end- or side-grafted at single or multiple sites of the chain.[7−10] If the end of a polymer chain is grafted onto a solid surface and the polymer is then stretched planar to the surface, it can cover a surface area as large as the projected area of the entire chain. Although extension of coil-like polymer chains usually incurs an entropic penalty, it is achieved at no energetic cost for rodlike polymers. In our previous study,[30,31] a SAM of planar rodlike polymers was produced on a mica surface by grafting an amphiphilic rod−coil block copolymer, poly(n-hexylisocyanate-*b*-2-vinylpyridine) (PHIC-*b*-P2VP), in which the P2VP block is a surface-active minority block and the PHIC block is a rodlike polymer. The PHIC chains were tethered to the surface via hydrogen bonding between the pyridine groups of the short P2VP block and the hydroxyl groups of the mica substrate. The PHIC chains formed a monolayer exhibiting a long-range nematic liquid crystalline order.

It should be noted that the rodlike chains, such as PHIC, can be regarded as one-dimensionally self-organized structures because their alkyl side groups are arranged along the rodlike backbone on the substrate surface. On the substrate surface, these rigid backbones are arranged parallel to one another,

Received: April 21, 2011
Revised: June 21, 2011
Published: July 11, 2011

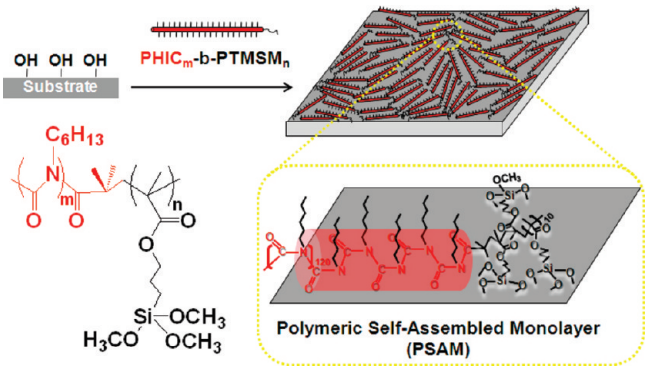

Figure 1. Schematic representation of the polymeric self-assembled monolayer (PSAM) prepared by grafting a rod−coil polymer consisting of a long rodlike block (with alkyl side groups) and a short sticky coil block (with a surface-reactive trimethoxysilyl groups).

producing a PSAM of two-dimensionally arranged alkyl side groups. Because the top surface of the resultant PSAM consists of alkyl groups, the surface energy of the PSAMs is likely to be similar to that of the SAMs prepared from alkylsilanes or alkane thiols.

However, the PSAM and small molecule SAM are distinct by several measures. In PSAMs, numerous alkyl side groups (as many as the degree of polymerization) are bound to a single polymer chain that is tethered to the surface only at the chain end. Because the end-grafted rodlike chains have rotational degrees of freedom in the polar and azimuthal angles, the area underneath the polymer chain may be exposed to the environment as the chain is desorbed from the surface. In contrast, in a small molecule SAM, each alkyl group is permanently bonded to the surface, and the surface beneath the SAM cannot be exposed unless the covalent bonds between the SAM and surface are cleaved. This distinction provides the PSAMs with unique properties, such as stimuli-responsiveness, which make them potentially useful for tailoring the properties of inorganic substrate surfaces or organic/inorganic interfaces.

For the PSAMs to be utilized in practical applications, it is essential that the thin monolayer must withstand thermal or chemical treatment during processing. In this regard, we performed a preliminary experiment with PHIC-*b*-P2VP that was known to form PSAM on mica surfaces via strong hydrogen bonding between the P2VP block and mica surfaces. Instead of mica, we attempted to form the PSAM on the surface of silica-based substrates (Si wafer or quartz) that are generally used in various applications. However, the resultant polymeric layers deposited on the silica surfaces were easily rinsed away by solvents due to the weak hydrogen bonding interactions between P2VP and silica. Covalent grafting is desired for the formation of solvent-resistant PSAM.

Here, we synthesized a new rod−coil diblock copolymer consisting of PHIC and poly[3-(trimethoxysilyl)propyl methacrylate] (PTMSM) blocks and created a covalently bonded monolayer on the silica substrates (Figure 1). Trimethoxysilyl groups of the short PTMSM block reacted with the oxide substrate surface to yield covalent PSAM of PHIC chains. The structural responses of the PSAMs to solvent vapor were investigated. A new type of mixed SAM with nanoscopic heterogeneity was created by reaction of the PSAMs with an additional SAM agent. We also demonstrated rapid photopatternability of the PSAMs and their applicability as an interfacial layer in organic field-effect transistors.

EXPERIMENTAL SECTION

Materials. N,N,N′,N″,N″-Pentamethyldiethylenetriamine (PMDETA; >99%, Aldrich), 3-(trimethoxysilyl)propyl methacrylate (TMSM; 98%, Aldrich), 2-bromoisobutanoyl bromide (2-BiB; 99%, Aldrich), and n-hexyl isocyanate (HIC; 97%, Aldrich) were dried over CaH_2 overnight and distilled under reduced pressure. Copper(I) bromide (CuBr 98%, Aldrich) was purified under nitrogen by stirring in glacial acetic acid, filtered, and washed with absolute ethanol and ethyl ether, then dried under vacuum. Anhydrous tetrahydrofuran (THF; DC Chemical Company) was freshly distilled under nitrogen from Na/benzophenone ketyl prior to use. Anhydrous methanol (MeOH; DC Chemical Company) was dried by refluxing in the presence of CaH_2 and distilled prior to use. Anhydrous toluene, 4′-pentyl-4-biphenylcarbonitrile (5CB; 98%, Aldrich), and octadecyltrimethoxysilane (ODTMS; 90%, Aldrich) were used as received.

Synthesis of PHIC-Br. Polymerization of HIC (3.115 g, 24.53 mmol) was carried out with activated sodium biphenyl amide (0.0248 g, 0.13 mmol) in THF in a break-seal glass apparatus under high vacuum at −98 °C for 70 min.[32] The polymer was end-capped by adding 2-BiB (0.1260 g, 0.76 mmol). The reaction mixture was poured into a large amount of hexane and methanol. The precipitated polymer was filtered and dried. ^{1}H NMR poly(n-hexylisocyanate) macroinitiator (300 MHz, $CDCl_3$): δ 3.66 (br, 2H; $-CH_2-N$), 1.29 (s, 8H; $(CH_2)_4$), 0.88 (s, 3H; CH_3).

Synthesis of PHIC-*b*-PTMSM. A typical ATRP procedure was as follows. PHIC-Br (0.1067 g, 0.0042 mmol), CuBr (0.0006 g, 0.0042 mmol), one droplet of PMDETA, and anhydrous toluene (2 mL) were transferred into a flame-dried Schlenk flask with a magnetic stir bar and a rubber septum under a stream of dry nitrogen gas. The mixture was stirred until a homogeneous solution (green color) was obtained. The TMSM monomer (0.1250 g, 0.5040 mmol), having previously been bubbled with nitrogen gas for 1 h, was then added via a gastight syringe. The flask was degassed by three freeze−pump−thaw cycles. The flask was then immersed in an oil bath thermostatted at 35 °C. After 60 h, the flask was removed from the bath, the reaction mixture was cooled, and anhydrous THF was added to dilute the polymer solution. The solution was transferred to a basic alumina column by syringe to remove the catalyst. The polymer was then precipitated in anhydrous methanol. The solids (0.1130 g) were isolated by filtration and dried in a vacuum desiccator at room temperature. ^{1}H NMR (300 MHz, $CDCl_3$): δ PHIC block: 3.66 (br, 2H; $-CH_2-N$), 1.29 (s, 8H; $(CH_2)_4$), 0.88 (s, 3H; CH_3). PTMSM block: 3.88 (t, 2H; $-COOCH_2-$), 3.58 (s, 9H; $Si(OMe)_3$), 1.72−1.89 (s, 4H; in main chain CH_2 and side chain propyl $C-CH_2-C$, 1.12, 1.02, 0.86 (s, 3H; isotactic, atactic, and syndiotactic $C-CH_3$ in methacryl unit), 0.68 (s, 2H; $Si-CH_2-C$).[33]

Preparation of PSAM on the Silica Substrate. The PSAM was prepared on the silica substrate by dissolving PHIC-*b*-PTMSM in anhydrous toluene to a concentration of 0.1 w/v%. The block copolymer solution was filtered through a 0.2 μm Teflon membrane filter. Oxygen plasma-treated silica substrates were immersed in the copolymer solution for 24 h at room temperature. The substrates were repeatedly rinsed with anhydrous toluene and dried under vacuum at room temperature.

Solvent Vapor annealing. The PSAM-coated substrates were placed near a vial filled with solvent in a closed chamber for 24 h. The plates were then dried by exposure to the atmosphere.

Fabrication of the LC Cell. The LC cells were fabricated by pairing two PSAM-coated substrates. Mylar films (thickness: 3.5 μm) were sandwiched between the two substrates. The cells were then sealed using epoxy glue, except at two edges. The nematic LC 4′-pentyl-4-biphenylcarbonitrile (5CB, [Cryst-(24 °C)-N-(36 °C)-I]) and the cells were heated to 40 °C on a heating plate. 5CB was then introduced at an opened edge and reached the substrate by capillary action, and the LC cell was sealed with glue. The cell was removed from the heating plate and cooled to room temperature.

Preparation of the Mixed SAM on the Silica Substrate. This was carried out in a nitrogen-purged glovebox. Hydroxlyated silica substrates (after O_2 plasma treatment) were immersed in a PHIC-*b*-PTMSM solution (~ 0.1 w/v%) for 24 h at room temperature, thoroughly rinsed with anhydrous toluene, and dried under N_2 flow for 6 h. The resulting substrates were immersed in ODTMS dissolved in anhydrous toluene (1 v/v%) for 1 h, followed by sequential sonication in anhydrous toluene to remove excess ODTMS molecules.

Micropatterning of PSAMs by Photolithography. The PSAM-treated substrate was irradiated with a UV lamp (254 nm, 1.55 mW/cm^2) for 10 s in air using a photomask with a stripe pattern containing 5 μm features. The resultant substrate was ultrasonically rinsed three times in THF for 20 min. The cleaned SAMs were then dried. The water condensation figures on the micropatterned PSAM were all taken on an optical microscope (Olympus BX51) equipped with temperature controlled stages (Linkam LTS 350) and temperature controller (Linkam TMS 94).

Fabrication of FETs Using the PSAM. Gate electrodes were formed from a heavily doped Si wafer onto which were deposited 300 nm thermally grown SiO_2 (capacitance C = 10 nF̃cm^2) as the gate dielectric. The substrates were modified with a PSAM, and the regioregular poly(3-hexylthiophene) (rr-P3HT) (Rieke Metal Inc., regioregularity: 98%, MW = 27.3k) was spin-cast from a 1.0 w/v% toluene solution to obtain a 50 nm thick film. The P3HT films were transferred to the vacuum chamber for thermal evaporation of 40 nm thick Au electrodes through a shadow mask. The channel length L and width W were 50 μm and 1.5 mm, respectively. All fabrication steps were conducted in a N_2-purged glove box, except for the preparation of the PSAM on the silica-based substrate.

Measurements. ^{1}H NMR spectra were measured using a JEOL JNMLA300WB using $CDCl_3$ as the solvent. Chemical shifts were measured with respect to tetramethylsilane (TMS) at 0 ppm. The molecular weights and molecular weight distributions of polymers were determined by SEC (Waters model 515). The SEC had four columns: HR 0.5, HR 1, HR 3, and HR 4. Waters Styragel columns run in series, and the pore sizes of the columns were 50, 100, 1000, and 10000 Å, respectively. A refractive index detector was used, calibrated relative to polystyrene standards (American Polymer Standard Corp.) THF was used as the mobile phase at a flow rate of 1.0 mL/min, and the temperature was fixed at 40 °C. X-ray photoelectron spectroscopy (XPS) was performed at a 90° takeoff angle using a Multilab 2000 (Thermo Electron Corporation) spectrometer with Mg Kα radiation (1253.6 eV) as an X-ray source in an ultrahigh vacuum (1.0×10^{-9}–1.0×10^{-10} mbar). The analyzed core level lines (C1s, O1s, N1s, Si2p) were calibrated with respect to the C1s binding energy set at 285 eV. Atomic force microscopy (AFM) investigations were performed using a commercial scanning probe microscope (Digital Instruments (DI) Multimode SPM IIIa system). The AFM was equipped with a Quadrex for phase imaging, and a Micro 40 active antivibration unit (Halcyonics) permitted better resolution. An etched silicon probe (RTESP) (Veeco probe) was used as the cantilever in tapping mode. The probes had force constants of 20–80 N/m, and resonance frequencies of 276–303 kHz. The cantilever was forced to oscillate near its resonance frequency. The laser beam was centered on the tip of the cantilever and reflected onto a photodiode. To minimize the sample surface deformation by the tip, the so-called light tapping method was applied. The electrical characteristics of OFET devices were measured in the saturation regime (VD = −60 V) using a Keithley 4200-SCS semiconductor parameter analyzer.

RESULTS AND DISCUSSION

Synthesis of Surface-Reactive Rod–Coil Block Copolymers. The macroinitiator, PHIC-Br, with a number-average molecular weight (Mn) of 15,900 and a polydispersity index of 1.10, was synthesized by living anionic polymerization of n-hexylisocyanate (HIC), followed by termination with 2-bromoisobutanoyl bromide (2-BiB), as reported previously (Figure 2).[32] Subsequent atom transfer radical polymerization (ATRP) with (3-trimethoxysilyl)propyl methacrylate (TMSM) was performed to yield PHIC-*b*-PTMSM (Figure 3). Polymerization at a high temperature near 90 °C resulted in depolymerization of the PHIC block, most likely due to reactions with the basic agents used for ATRP.[34] To avoid the base-catalyzed depolymerization of PHIC, the polymerization reaction was conducted under mild reaction conditions at 35 °C in toluene. A large excess of TMSM induced the PTMSM chain to grow from the PHIC-Br macroinitiator, even under the mild conditions. The composition of the block copolymer was analyzed by comparing the ^{1}H NMR and size exclusion chromatography–light scattering (SEC-LS) data of PHIC-Br and the block copolymer. The block copolymers obtained from several ATRP runs always had a TMSM weight fraction less than 20%. It has been reported that ATRP of TMSM monomer from other types of macroinitiator gives a block copolymer with a minority PTMSM block (5–10%) in spite of the use of an excess amount of monomer.[35,36] Table 1 shows the two block copolymers used for PSAM formation. This asymmetric composition was ideal for producing a surface-tethered PHIC monolayer.

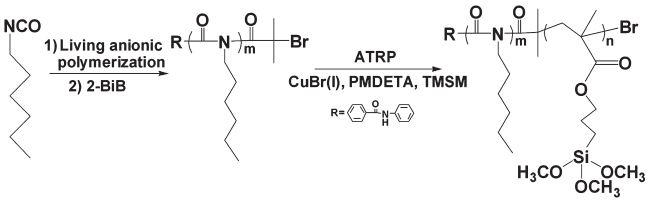

Figure 2. Synthesis of PHIC$_m$-*b*-PTMSM$_n$.

PSAM Coating. The PHIC-*b*-PTMSM block copolymer was coated onto clean wafer or quartz plates by immersion coating from their toluene solutions. The substrates could be fully covered with a PSAM over a wide immersion solution concentration range, between 0.005 and 2 w/v%. After serveral hours of immersion, the water contact angle of the PSAM-coated silica substrate approached 100°, comparable to that observed for alkyl SAMs (Figure 4). A copolymer concentration of 0.1 w/v% in toluene with an immersion time of 24 h at room temperature was convenient. The excess block copolymers physically adsorbed to the PSAM layer could be removed by washing and ultrasonication in solvent to yield uniform PSAMs.

The surface morphology of the PSAM was investigated by atomic force microscopy (AFM) (Figure 5). The PSAM surface was smooth over a large area with a root-mean-square (rms) roughness less than 0.3 nm (Figure 5a). The thickness of the polymer layer was determined from an AFM image of a sample softly scratched with a razor blade (Figure 5b). The thickness of the film was 1.2–1.5 nm, close to the known diameter of PHIC.[37] This result suggests that the PHIC chains are aligned parallel to the substrate surface. A nematic liquid crystal, 4′-pentyl-4-biphenylcarbonitrile (5CB), exhibited homeotropic alignment between two PSAM-coated substrates (Figure S1 of the Supporting Information). These data support that the hexyl side chains along the PHIC backbone are oriented perpendicular to the substrate surface.[38]

Covalent bonding of the PHIC chains on the substrate was confirmed by X-ray photoelectron spectroscopy (XPS) of the

Table 1. Molecular Weight Characteristics of PHIC-*b*-PTMSM

			block composition		
polymer	M_n of PHIC[a]	M_n of PTMSM[b]	wt % of PHIC	wt % of PTMSM	PDI
$PHIC_{125}$-*b*-$PTMSM_{12}$	15,900	3000	84	16	1.23
$PHIC_{125}$-*b*-$PTMSM_6$	15,900	1500	91	9	1.18

[a] M_n of PHIC was measured by size exclusion chromatography−light scattering (SEC-LS) calibrated with polystyrene standards in a THF solution containing 2% triethylamine as the eluent at 40 °C. [b] The M_n of PTMSM was estimated by ^{1}H NMR integration.

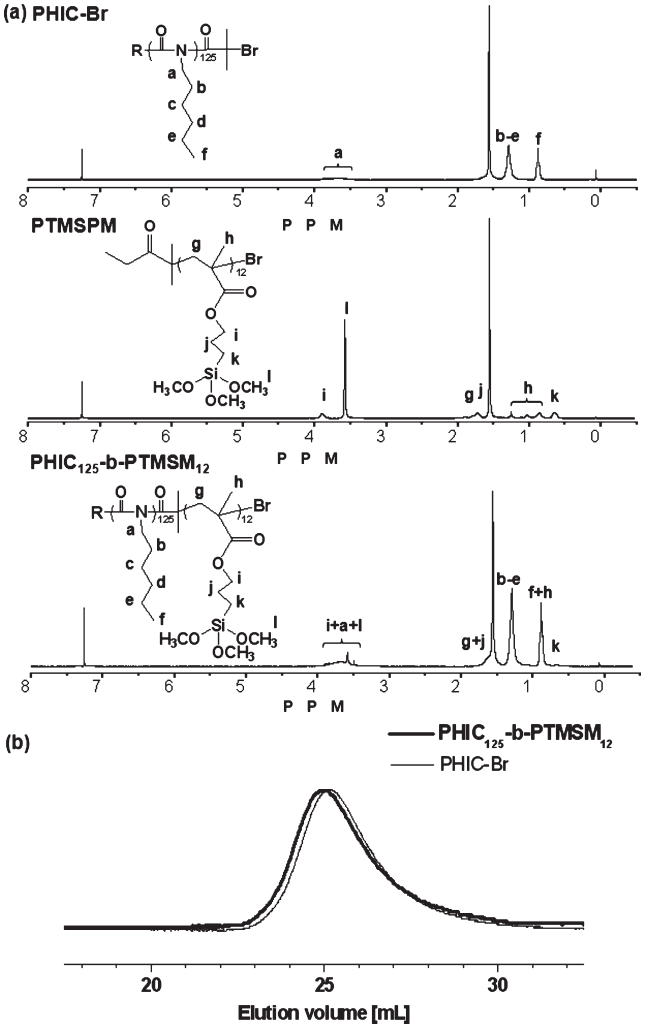

Figure 3. (a) ^{1}H NMR spectra of PHIC-Br, PTMSM, and $PHIC_{125}$-*b*-$PTMSM_{12}$ in $CDCl_3$. (b) SEC profiles of PHIC-Br and $PHIC_{125}$-*b*-$PTMSM_{12}$.

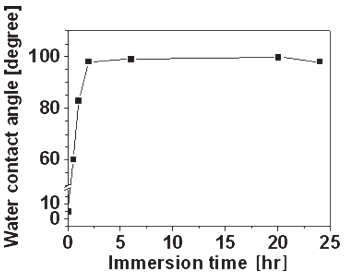

Figure 4. Water contact angle of PSAM with increasing immersion coating time in the 0.1w/v% toluene solution.

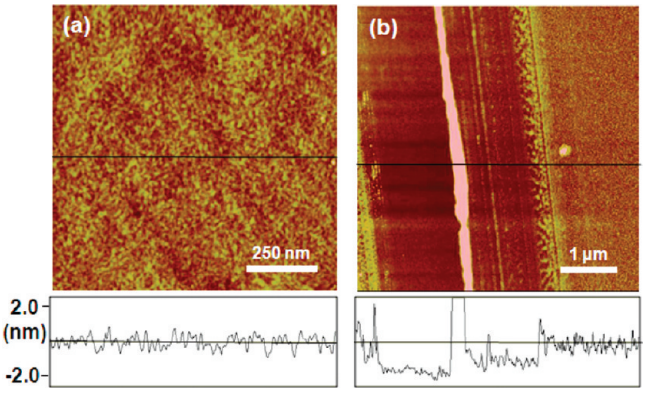

Figure 5. Surface morphology and thickness of a PSAM. (a) PSAM height contrast was measured by tapping mode AFM. The PSAM was prepared on a silica substrate by immersion for 1 day in a 0.1 w/v% toluene solution, followed by ultrasonic washing. (b) Height contrast TM AFM image of a PSAM scratched with a razor blade.

PSAM-coated substrate washed with solvent. Even after ultrasonic cleaning in solvent, the PSAM exhibited an N1s peak centered at a binding energy of 400.7 eV, corresponding to the PHIC amide group. A control experiment involving the PHIC homopolymer without surface-reactive moieties demonstrated that immersion of the substrate, followed by ultrasonic washing, yielded only a negligible N1s peak in the XPS data (Figure 6). Only covalently bound PHIC chains formed stable PSAMs.

The uniform thickness and morphology of the PSAMs regadless of different concentrations and immersion times indicate that covalent adsorption of the copolymer chains onto the substrate was self-limiting. In other words, the grafting reaction of the copolymer chains to the surface ceased as the surface became saturated with the PSAM. The PHIC chains tethered to the surface by short PTMSM chains formed a protective layer to prevent further access of the polymers to the surface. Because of this self-limiting coating mechanism, uniform PSAM film can be prepared reproducibly onto large substrates by simple procedures using various concentrations and immersion times.

Assuming the substrate surface is fully covered with the planar PHIC monolayer, the surface area covered by a single PHIC chain is estimated to be approximately 30 nm^2, as obtained by multiplying the length of the extended PHIC chain (the repeating unit length,[39] 0.2 nm, times the degree of polymerization (DP), 125) by the diameter of the PHIC chain (1.2 nm). Covering the same area with an alkyl SAM derived from small molecules, such as octadecyltriethoxysilane (ODTE) or octadecyltrichlorosilane (ODTS), would require close alignment of the

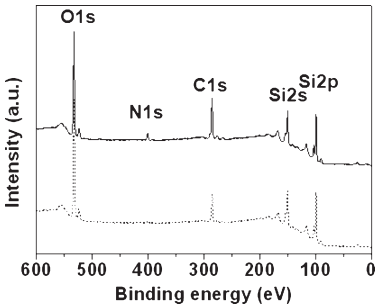

Figure 6. X-ray photoelectron spectroscopy (XPS) spectrum of $PHIC_{125}$-*b*-$PTMSM_{12}$ (solid line) and PHIC-Br with no surface-reactive groups (dashed line) on a silica substrate after rinsing and sonication.

molecules as many as the number of repeating units constituting a single PHIC chain.[40,41] This comparison indicates that the surface area covered by the PSAM per grafting site is about 2 orders of magnitude greater than that by small alkyl SAM molecules.

Morphological Response of PSAMs to Solvent Vapor. Because the rodlike polymer chains are bound to the surface only by their chain ends, the chains in the PSAM have freedom in their rotational motion. The rodlike chains can order parallel to one another to form a liquid crystalline monolayer. We investigated the reorganization of the end-tethered PHIC chains in the PSAM by annealing in an atmosphere saturated with THF, chloroform, toluene, or hexane, all of which are good solvents for PHIC. After annealing the PSAM with THF or chloroform vapor, the defect texture typical to nematic liquid crystals such as splay and bend deformation of director appeared in the AFM image (Figure 7), whereas no such LC texture was observed in the PSAM treated under toluene or hexane vapor. The LC texture observed in the dry PSAM indicates that the PHIC chains form a lytropic nematic state when swollen with the solvent vapor as observed previously in PHIC-*b*-P2VP block copolymer.[30,31] Although toluene and hexane are good solvents for PHIC in the bulk solution phase, they are relatively hydrophobic and may not easily break the interactions between the PHIC amide backbone and the hydrophilic substrate surface. Reorganization of the PHIC chains would, therefore, be prohibited in more hydrophobic solvents.

Preparation of a Mixed SAM by Coating of an alkyl SAM onto the PSAM. In general, a substrate surface fully covered with a covalently bonded SAM composed of small molecules cannot be functionalized by further addition of other SAM-forming agents. The surfaces with multiple functionalities are usually obtained by transforming some of the functional groups in the tail of SAM molecules into a different chemical structure.[42] In contrast, the PSAM-coated surface investigated here can accommodate additional SAM-forming surface-reactive agents because much of the surface underneath the PSAM is still available for covalent grafting. The unreacted surface beneath the rodlike polymer chains may be exposed to a solution containing additional surface-reactive agents to yield a mixed SAM.[30,31]

Octadecyltrimethoxysilane (ODTMS) was used as a second SAM agent to the PSAM. As the PSAM-coated substrate of Figure 7 was immersed in a solution containing 1 v/v% ODTMS in toluene, followed by rinsing with solvent, a random dot pattern of octadecyl SAM was obtained, as shown in Figure 8. The size of nanodots grew initially and then saturated after immersion time of about 30 min, indicating that the growth of ODTMS SAM was also limited by the PSAM. The heights of the dots were

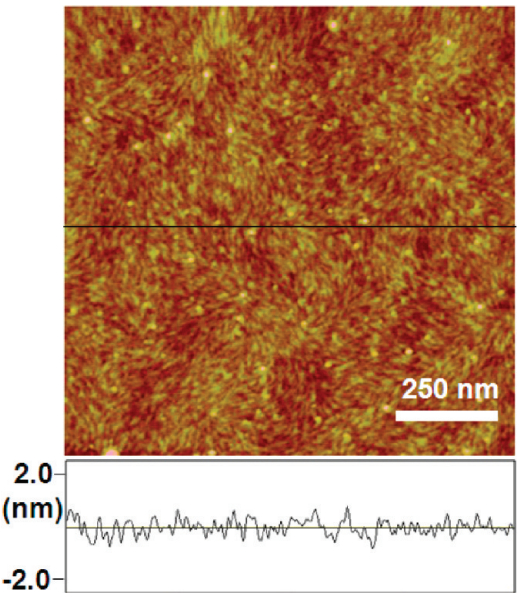

Figure 7. TM AFM height image and height profiles of the PSAM annealed in THF vapor for 24 h.

2.4−2.8 nm, and the widths were 20−30 nm, as determined from the TM AFM height image. The heights were comparable to the extended chain length of the ODTMS.[43] Shorter alkyl SAM agents, such as octyl TMS, did not produce a dot pattern, most likely because the short alkyl chains produced nanodot domains with a height contrast lower than that observed for the PSAM regions.

The nanodot pattern formation may be attributed to the confined adsorption and reaction of alkyl SAM agent on the PSAM surface. Upon immersion of PSAM-coated subsrate into a second SAM agent solution, the grafted PHIC blocks are fluidized via formation of either a lyotropic liquid crystalline solution (Figure 8e) or an isotropic solution state. Alkyl SAM agents approach the substrate surface by way of disordered domains or exposed surface regions, from which alkyl SAMs nucleate and grow to a nanoscopic size until limited by the PSAM chains. The formation of uniformly distributed nanodot patterns on the PSAM surface is a promising technique for preparing chemically heterogeneous surface with functional nanoscopic domains.

Micropatterning of PSAM. The backbone and side groups of the polymethacrylate chains may undergo scission when irradiated with UV.[44,45] The anchoring moiety of the PHIC-*b*-PTMSM is a polymethacrylate, and therefore, the covalent bonds may be cleaved photochemically. Photochemical cleavage of the methacrylates moieties in the PSAM was found to be complete within 10 s using an ordinary 254 nm 1.55mW/cm^2 UV lamp (Figure 9a). UV exposure time was optimized by evaluating water condensation figure on the micropatterned PSAM with different UV irradiation time (Figure 10). Micropatterned PSAMs were prepared by UV (254 nm) irradiation of the PSAM through a photomask, followed by ultrasonic cleaning in a solvent (Figure 9b). It should be noted that the conditions used for micropatterning of the PSAM were much milder than those used to create alkyl SAM patterns on a silica substrate.[46−49] The AFM image of the resultant micropatterned PSAM is shown in panel (c) of Figure 9. In a control experiment, we compared the XPS data of PSAM, UV-treated PSAM and silica, which indicated

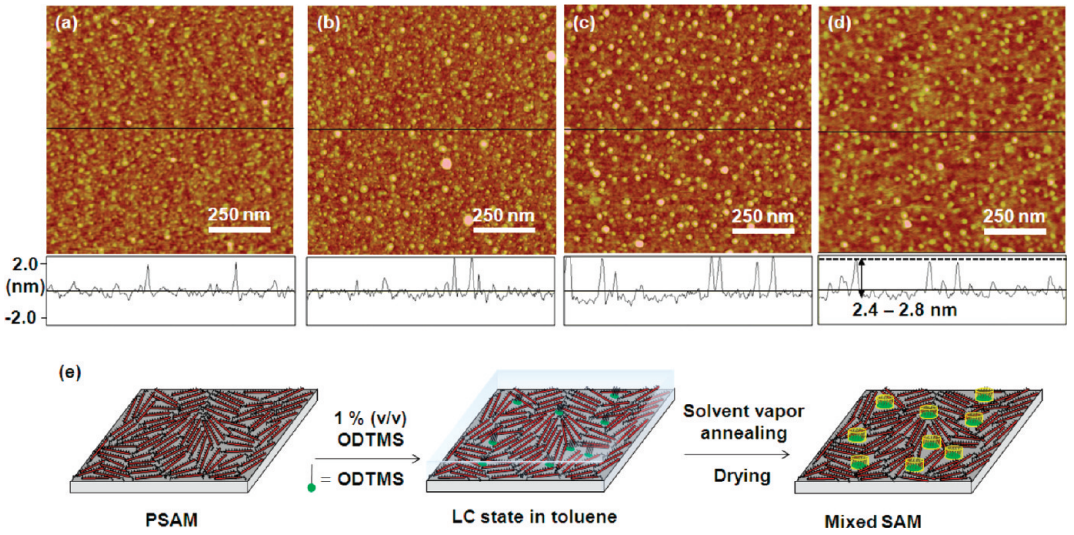

Figure 8. Height contrast TM AFM image of a mixed SAM after immersion in the second SAM agent solution for (a) 10 min, (b) 20 min, (c) 30 min, and (d) 60 min. (e) Schematic drawings representing the formation of an alkyl/polymer mixed PSAM.

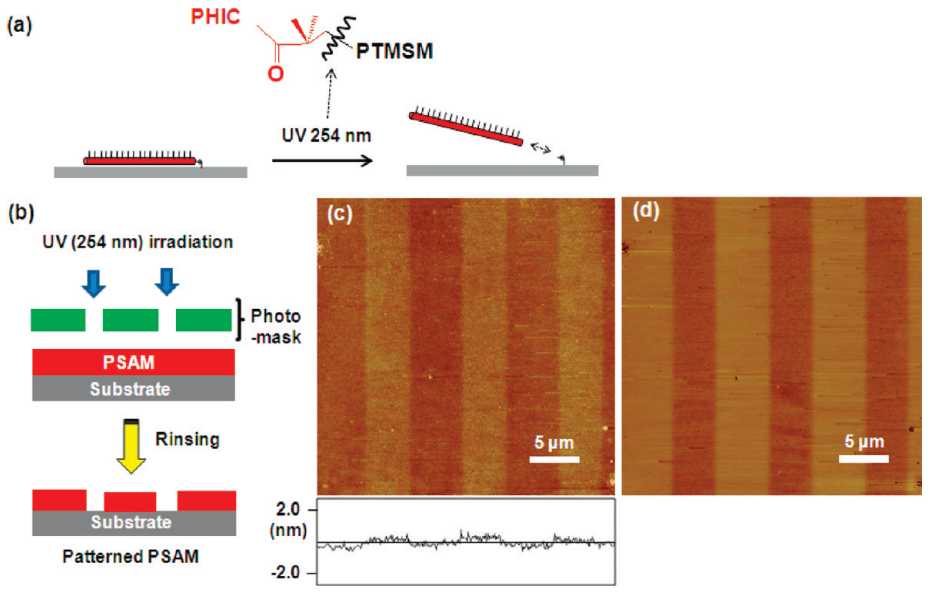

Figure 9. (a) Photochemical cleavage of the PSAM from the surface by UV irradiation. (b) Schematic illustration showing the photopatterning of the PSAM. (c,d) Height and phase contrast TM AFM image, respectively, of a micropatterned PSAM.

that the C_{1s} peak intensity was substantially reduced by UV treatment, to a level as low as that of a bare silica surface, as the pristine PSAM was irradiated only for 10 s with UV (Figure 11). After UV irradiation of the PSAM, the C_{1s} peaks at 281.7 and 286.6 eV, corresponding to C−Si and C−O bonds, respectively, were still observed in its XPS data (Figure 11 , Figure S2 and Table S1 of the Supporting Information), whereas, the peaks for ester or amide carbonyl carbons were negligible. This means that the polymer backbones were completely removed even by the brief UV irradiation while forming the alkyl silica residues. The high sensitivity of the PSAM to the UV is likely due to ultrathin thickness as well as low grafting density of the PSAM. The substrate suface underneath a planar macromolecular chain is exposed by photocleavage of the chain end as represented in panel (a) of Figure 9.

Application of PSAM in FETs. To test the applicability of the PSAM in organic electronics, we utilized the PSAM as an additional dielectric layer in P3HT-based field effect transistors (FETs) (Figure 12). FETs prepared on the PSAM-coated SiO_2/Si substrate exhibited a charge carrier mobility (μ) = $1.7 \pm 0.5 \times 10^{-3}$ cm^2 V^{-1} s^{-1}, which was 1 order of magnitude higher than that of the untreated silica dielectric layer ($2.3 \pm 0.7 \times 10^{-4}$ cm^2 V^{-1} s^{-1}). The performance of the PSAM-treated device was lower than that of the octadecyltrichlorosilane (ODTS)-treated device ($1.0 \pm 0.5 \times 10^{-2}$ cm^2 V^{-1} s^{-1}). The lower performance of the PSAM-treated FET as compared with the ODTS-treated one may be accounted for by the shorter hexyl side group of PHIC chains constituting the PSAM than the octadecyl SAM. It has been reported that FETs on the shorter alkyl SAMs exhibit lower mobilities than those on the longer alkyl SAMs.[50]

dx.doi.org/10.1021/cm201138u |*Chem. Mater.* 2011, 23, 3517–3524

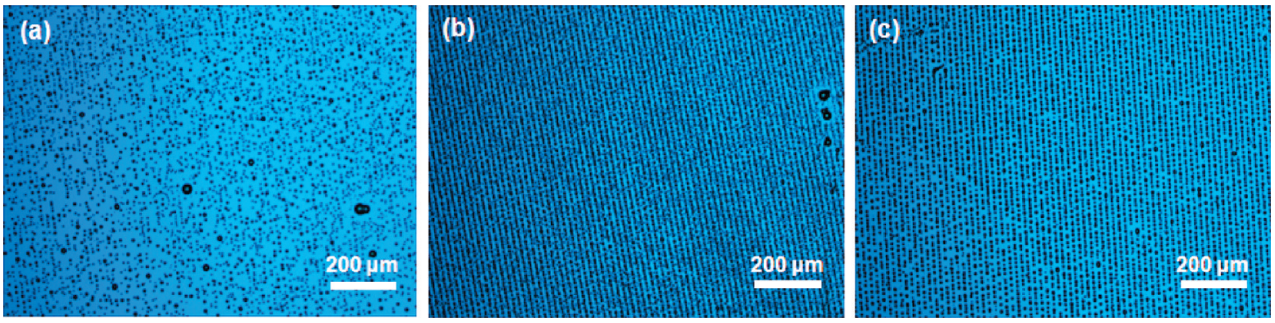

Figure 10. Optical microscope images of water condensation figures on the micropatterned PSAM obtained by UV exposure for (a) 1 s, (b) 5 s, and (c) 10 s.

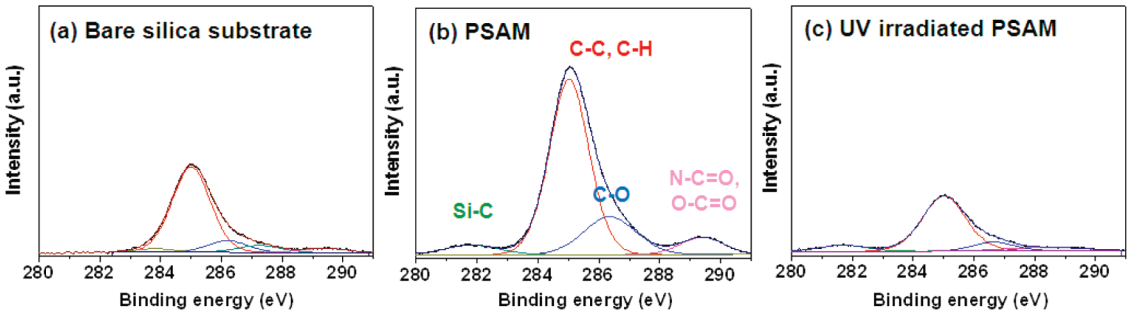

Figure 11. XPS analysis of the C(1s) core-level spectrum of (a) a bare silica surface, (b) as-prepared PSAM, and (c) PSAM treated with UV 254 nm.

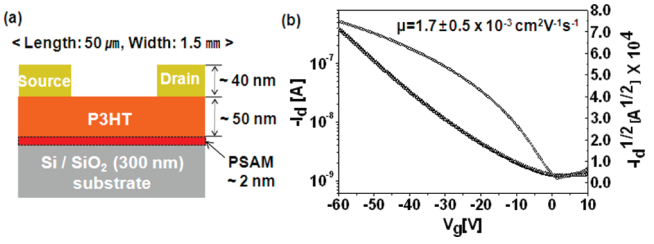

Figure 12. Fabrication of P3HT-based FETs using PSAM. (a) Structural geometry of the FET prepared using a PSAM. (b) Transfer characteristics of the PSAM-treated FET.

Neverthless, the result indicates that the PSAM can be used as an interfacial layer in organic electronic applications with qualities comparable to those of the alkyl SAMs.

CONCLUSIONS

In summary, a surface-reactive rod−coil diblock copolymer consisting principally of a rodlike polymer block (PHIC) with a surface reactive block (PTMSM) was synthesized by living anionic polymerization and the ATRP method. Simple immersion coating of the rod−coil polymer onto the silica substrates provided a PSAM consisting of a planar adsorbed PHIC monolayer with PTMSM anchors. Thanks to the rotational freedom of the end-grafted PHIC chains, the PSAMs exhibited liquid crystalline ordering in the presence of solvent vapor and yielded a mixed SAM consisting of nanodot-like alkyl SAMs and PSAMs. Photochemical micropatterning of the PSAM was accomplished using conventional UV photolithography. The micropatterning process used a much smaller total power and a shorter irradiation time in comparison with the micropatterning process of conventional alkyl SAMs. The P3HT FET device fabricated using a PSAM interfacial dielectric layer exhibited a performance similar to that of a device prepared with an alkyl SAM.[51,52]

We demonstrated that the PSAMs exhibited unique properties not generally observed in small molecule SAMs. These properties included a low grafting density, responsiveness to solvents, reactivity toward additional surface-functionalizing reagents, the ability to form a mixed SAM with a nanoscopic pattern, and rapid photopatternability.

The simple processing conditions, such as the concentration window and the immersion time for preparing a uniform nanometer-thick PSAM, are advantageous in comparison with the conditions required by other SAM materials. Further studies of PSAMs composed of other functional polymers, such as conjugated polymers or biological polymers, will be promising.

ASSOCIATED CONTENT

Supporting Information. OM image of homeotropically aligned LC between PSAMs and schematic structure of a LC cell; and XPS survey spectra of bare silica substrate, PSAM, micropatterned PSAM, and UV irradiated whole surface of PSAM with detailed surface elemental composition. This material is available free of charge via the Internet at http://pubs.acs.org.

AUTHOR INFORMATION

Corresponding Author

*E-mail: jiwoong@gist.ac.kr.

ACKNOWLEDGMENT

This work was supported by a Korea Science and Engineering Foundation (KOSEF) grant [2010-0000282 and 2010-0026421]

funded by the Korean government (MEST) and the Program for Integrated Molecular System at GIST.

REFERENCES

(1) Ulman, A. *Chem. Rev.* **1996**, *96*, 1533–1554.
(2) Fendler, J. H. *Chem. Mater.* **2001**, *13*, 3196–3210.
(3) Love, J. C.; Estroff, L. A.; Kriebel, J. K.; Nuzzo, R. G.; Whitesides, G. M. *Chem. Rev.* **2005**, *105*, 1103–1169.
(4) Haensch, C.; Hoeppener, S.; Schubert, U. S. *Chem. Soc. Rev.* **2010**, *39*, 2323–2334.
(5) Bhat, R.; Sell, S.; Wagner, R.; Zhang, J. T.; Pan, C.; Garipcan, B.; Boland, W.; Bossert, J.; Klemm, E.; Jandt, K. D. *Small* **2010**, *6*, 465–470.
(6) Gutzler, R.; Sirtl, T.; Dienstmaier, J. r. F.; Mahata, K.; Heckl, W. M.; Schmittel, M.; Lackinger, M. *J. Am. Chem. Soc.* **2010**, *132*, 5084–5090.
(7) Park, J.-W.; Kim, H.; Han, M. *Chem. Soc. Rev.* **2010**, *39*, 2935–2947.
(8) Stuart, M. A. C.; Huck, W. T. S.; Genzer, J.; Muller, M.; Ober, C.; Stamm, M.; Sukhorukov, G. B.; Szleifer, I.; Tsukruk, V. V.; Urban, M.; Winnik, F.; Zauscher, S.; Luzinov, I.; Minko, S. *Nat. Mater.* **2010**, *9*, 101–113.
(9) Zhou, F.; Huck, W. T. S. *Phys. Chem. Chem. Phys.* **2006**, *8*, 3815–3823.
(10) Paik, M. Y.; Xu, Y.; Rastogi, A.; Tanaka, M.; Yi, Y.; Ober, C. K. *Nano Lett.* **2011**, *10*, 3873–3879.
(11) Khanduyeva, N.; Senkovskyy, V.; Beryozkina, T.; Horecha, M.; Stamm, M.; Uhrich, C.; Riede, M.; Leo, K.; Kiriy, A. *J. Am. Chem. Soc.* **2008**, *131*, 153–161.
(12) Kramarenko, E. Y.; Potemkin, I. I.; Khokhlov, A. R.; Winkler, R. G.; Reineker, P. *Macromolecules* **1999**, *32*, 3495–3501.
(13) Paoprasert, P.; Spalenka, J. W.; Peterson, D. L.; Ruther, R. E.; Hamers, R. J.; Evans, P. G.; Gopalan, P. *J. Mater. Chem.* **2010**, *20*, 2651–2658.
(14) In, I.; La, Y.-H.; Park, S.-M.; Nealey, P. F.; Gopalan, P. *Langmuir* **2006**, *22*, 7855–7860.
(15) Park, J. W.; Thomas, E. L. *J. Am. Chem. Soc.* **2002**, *124*, 514–515.
(16) Park, J.-W.; Cho, Y.-H. *Langmuir* **2006**, *22*, 10898–10903.
(17) Kumaki, J.; Hashimoto, T. *J. Am. Chem. Soc.* **2003**, *125*, 4907–4917.
(18) Yoon, B.; Huh, J.; Ito, H.; Frommer, J.; Sohn, B. H.; Kim, J. H.; Thomas, E. L.; Park, C.; Kim, H. C. *Adv. Mater.* **2007**, *19*, 3342–3348.
(19) Park, S.; Lee, K. B.; Choi, I. S.; Langer, R.; Jon, S. *Langmuir* **2007**, *23*, 10902–10905.
(20) Luzinov, I.; Minko, S.; Tsukruk, V. V. *Prog. Polym. Sci.* **2004**, *29*, 635–698.
(21) Azzaroni, O.; Brown, A. A.; Huck, W. T. S. *Angew. Chem., Int. Ed.* **2006**, *118*, 1802–1806.
(22) Yang, S. Y.; Kim, D. Y.; Jeong, S. M.; Park, J. W. *Macromol. Rapid Commun.* **2008**, *29*, 729–736.
(23) Cheng, L.; Cao, D. *ACS Nano* **2011**, *5*, 1102–1108.
(24) Santer, S.; Kopyshev, A.; Donges, J.; Yang, H. K.; Rühe, J. *Adv. Mater.* **2006**, *18*, 2359–2362.
(25) Zhao, B.; Haasch, R. T.; MacLaren, S. *J. Am. Chem. Soc.* **2004**, *126*, 6124–6134.
(26) Krishnamoorthy, S.; Pugin, R.; Brugger, J.; Heinzelmann, H.; Hinderling, C. *Adv. Funct. Mater.* **2006**, *16*, 1469–1475.
(27) Julthongpiput, D.; Lin, Y. H.; Teng, J.; Zubarev, E. R.; Tsukruk, V. V. *J. Am. Chem. Soc.* **2003**, *125*, 15912–15921.
(28) Motornov, M.; Sheparovych, R.; Lupitskyy, R.; MacWilliams, E.; Hoy, O.; Luzinov, I.; Minko, S. *Adv. Funct. Mater.* **2007**, *17*, 2307–2314.
(29) Wu, T.; Gong, P.; Szleifer, I.; Vlccek, P.; Subr, V.; Genzer, J. *Macromolecules* **2007**, *40*, 8756–8764.
(30) Kim, J.-H.; Rahman, M. S.; Lee, J.-S.; Park, J.-W. *J. Am. Chem. Soc.* **2007**, *129*, 7756–7757.
(31) Kim, J.-H.; Rahman, M. S.; Lee, J.-S.; Park, J.-W. *Macromolecules* **2008**, *41*, 3181–3189.
(32) Rahman, M. S.; Samal, S.; Lee, J.-S. *Macromolecules* **2006**, *39*, 5009–5014.
(33) Du, J.; Chen, Y. *Macromolecules* **2004**, *37*, 6322–6328.
(34) Khatri, C. A.; Vaidya, M. M.; Levon, K.; Jha, S. K.; Green, M. M. *Macromolecules* **1995**, *28*, 4719–4728.
(35) Huang, J.; Koepsel, R. R.; Murata, H.; Wu, W.; Lee, S. B.; Kowalewski, T.; Russell, A. J.; Matyjaszewski, K. *Langmuir* **2008**, *24*, 6785–6795.
(36) Yu, H.; Wang, L.; Chen, T. *Eur. Polym. J.* **2009**, *45*, 639–642.
(37) Ohkita, M.; Higuchi, M.; Kawaguchi, M. *J. Colloid Interface Sci.* **2005**, *292*, 300–303.
(38) Malone, S. M.; Schwartz, D. K. *Langmuir* **2008**, *24*, 9790–9794.
(39) Fetters, L. J.; Yu, H. *Macromolecules* **1971**, *4*, 385–389.
(40) Allara, D. L.; Parikh, A. N.; Judge, E. *J. Chem. Phys.* **1994**, *100*, 1761–1764.
(41) Tian, F.; Xiao, X.; Loy, M. M. T.; Wang, C.; Bai, C. *Langmuir* **1999**, *15*, 244–249.
(42) Bhat, R.; Sell, S.; Trimbach, D. C.; Zankovych, S.; Zhang, J.; Bossert, J. r.; Klemm, E.; Jandt, K. D. *Chem. Mater.* **2008**, *20*, 5197–5202.
(43) Ito, Y.; Virkar, A. A.; Mannsfeld, S.; Oh, J. H.; Toney, M.; Locklin, J.; Bao, Z. *J. Am. Chem. Soc.* **2009**, *131*, 9396–9404.
(44) Hiraoka, H. *IBM J. Res. Dev.* **1977**, *21*, 121–130.
(45) Horiuchi, S.; Fujita, T.; Hayakawa, T.; Nakao, Y. *Adv. Mater.* **2003**, *15*, 1449–1452.
(46) Lin, Y.-C.; Yu, B.-Y.; Lin, W.-C.; Chen, Y.-Y.; Shyue, J.-J. *Chem. Mater.* **2008**, *20*, 6606–6610.
(47) Sugimura, H.; Ushiyama, K.; Hozumi, A.; Takai, O. *Langmuir* **2000**, *16*, 885–888.
(48) Herzer, N.; Hoeppener, S.; Schubert, U. S. *Chem. Commun.* **2010**, *46*, 5634–5652.
(49) Hong, L.; Sugimura, H.; Furukawa, T.; Takai, O. *Langmuir* **2003**, *19*, 1966–1969.
(50) Horii, Y.; Ikawa, M.; Sakaguchi, K.; Chikamatsu, M.; Yoshida, Y.; Azumi, R.; Mogi, H.; Kitagawa, M.; Konishi, H.; Yase, K. *Thin Solid Films* **2009**, *518*, 642–646.
(51) Choi, D.; Jin, S.; Lee, Y.; Kim, S. H.; Chung, D. S.; Hong, K.; Yang, C.; Jung, J.; Kim, J. K.; Ree, M.; Park, C. E. *ACS Appl. Mater. Interfaces* **2009**, *2*, 48–53.
(52) Zen, A.; Pflaum, J.; Hirschmann, S.; Zhuang, W.; Jaiser, F.; Asawapirom, U.; Rabe, J. P.; Scherf, U.; Neher, D. *Adv. Funct. Mater.* **2004**, *14*, 757–764.